JOC The Journal of Organic Chemistry

Article

pubs.acs.org/joc

Time- and Concentration-Dependent Reactivity of Cys, Hcy, and GSH on the Diels–Alder-Grafted 1,3,5-Tris Conjugate of Calix[6]arene To Bring Selectivity for Cys: Spectroscopy, Microscopy, and Its Reactivity in Cells

V. V. Sreenivasu Mummidivarapu, Deepthi S. Yarramala, Karuna Kumar Kondaveeti, and Chebrolu P. Rao*

Bioinorganic Laboratory, Department of Chemistry, Indian Institute of Technology Bombay, Powai, Mumbai 400 076, India

Supporting Information

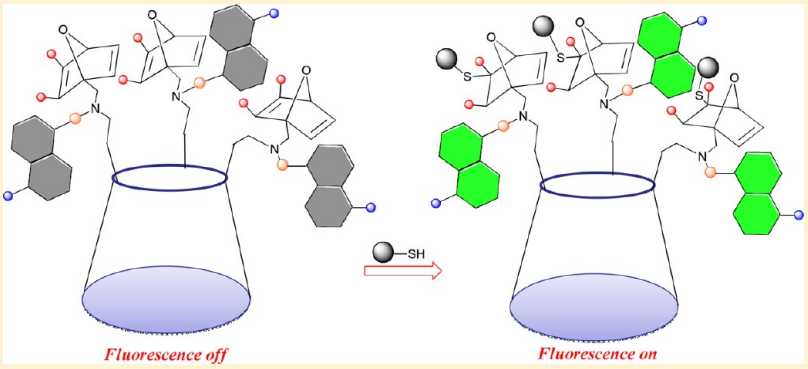

ABSTRACT: Herein we report the synthesis and characterization of 7-oxanorbornadiene (OND)-appended 1,3,5-tris conjugate of calix[6]arene ($\mathbf{L_2}$). $\mathbf{L_2}$ has been shown to exhibit selective reactivity toward cysteine (Cys) over homocysteine (Hcy) and glutathione (GSH) under stoichiometric conditions. The selectivity of $\mathbf{L_2}$ is attributed to the steric crowding of three Diels–Alder centers possessing OND units present on the calix[6]arene platform, while a control molecular system possessing only one such unit without the calix[6]arene platform ($\mathbf{L_1}$) does not show any selectivity toward Cys. While $\mathbf{L_2}$ exhibited spherical particles, its reactivity with Cys resulted in flowerlike morphological features, as revealed by scanning electron microscopy. However, the reaction with GSH did not result in any such morphological features, a result that is in agreement with that observed from fluorescence studies in solution. $\mathbf{L_2}$ has been shown to react with Cys present in HeLa and Jurkat E6 cells by fluorescence microscopy.

INTRODUCTION

Biological thiols (BTs) play essential roles in reversible redox reactions.[1] Cysteine (Cys) is involved in protein synthesis and acts as a potential neurotoxin.[2] Deficiency of Cys leads to slow growth, hair depigmentation, decrease in hematopoiesis, loss of leucocytes, liver damage, and weakness.[3] Elevated levels of homocysteine (Hcy) in plasma lead to disorders such as cardiovascular and Alzheimer's diseases, pregnancy-related complications, inflammatory bowel disease, and osteoporosis.[4] Since the imbalance of both Cys and Hcy in biological systems lead to disorders, these need to be discriminated via their differential interactions by a given molecular probe.[5] In recent years, efforts have been directed to the selective detection of thiols by probes possessing moieties such as disulfide cleavage, maleimide, 2,4-dinitrobenzenesulfonyl, chromophoric, and fluorophoric types.[6] In designing a probe that is selective for Cys over Hcy and glutathione (GSH), the following are noteworthy. GSH is a tripeptide in which the thiol-possessing Cys is the central residue, and the reactivity of the SH group is thus expected to be reduced as a result of steric crowding.[7] On the other hand, the SH in Cys is relatively more acidic than that in other thiols, suggesting a higher nucleophilic reactivity for Cys.[8,9] Inside the cell, the concentration of GSH (1–10 mM)[10a] is 30–50 times greater than that of Cys (30–200 μM).[10b,c] This presents a big challenge to the chemical detection strategies being developed for thiols. Therefore, a system that is initially nonfluorescent but possesses a sterically hindered electrophilic center that is selective for Cys among BTs in stoichiometric reactions is desirable. It would be indispensable if it could produce a large fluorescence enhancement as a result of the reaction of Cys compared with other BTs. Keeping all of these factors in mind, herein we report the synthesis of a 1,3,5-tris conjugate of calix[6]arene with 7-oxanorbornadiene (OND) appended on the lower rim ($\mathbf{L_2}$) for selective recognition of Cys under stoichiometric

Received: September 15, 2014
Published: October 13, 2014

Scheme 1. Synthesis of L_1[a]

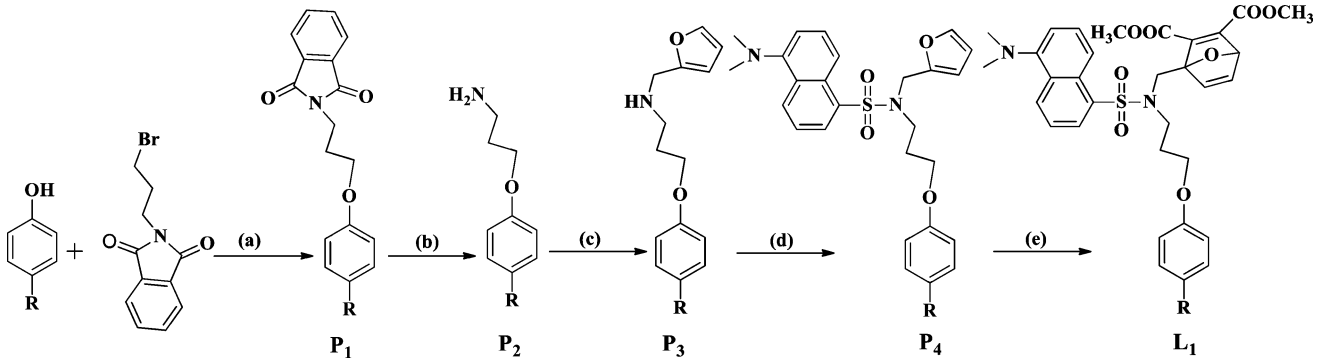

[a]R = *tert*-butyl. Reagents and conditions: (a) 3-bromopropylphthalimide, Cs_2CO_3, K_2CO_3, CH_3CN, 70 °C, 24 h; (b) NH_2–NH_2, C_2H_5OH, 80 °C, 12 h; (c) furfural, $NaBH_4$, CH_3OH, 24 h, rt; (d) dansyl chloride, Et_3N, from 0 °C to rt, 12 h; (e) dimethyl acetylenedicarboxylate (DMAD), dry CH_2Cl_2, 55 °C, 12 h.

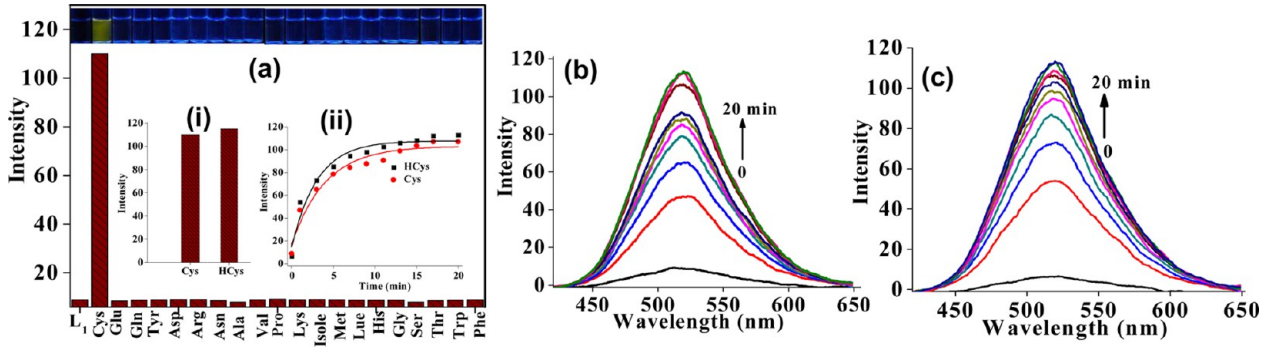

Figure 1. Fluorescence titrations of L_1 with AAs and Hcy. (a) Histogram showing the fluorescence intensities of L_1 (5 μM) in the presence of AAs (50 μM). Inset (i): intensity histogram. Inset (ii): plots of fluorescence intensity vs time at an L_1:AA ratio of 1:20. Inset (vials): colorimetric titrations of L_1 (5 μM) with different AAs (80 μM) in acetonitrile under 365 nm light. (b, c) Time-dependent fluorescence spectra of L_1 with 1 equiv of (b) Cys and (c) Hcy.

conditions compared with Hcy and GSH. Interactions of L_2 with thiols have been monitored by fluorescence and ^{1}H NMR spectroscopy, and the species generated during the reaction were detected by ESI MS. Entry of L_2 into cells followed by its reaction with cellular thiols has also been demonstrated. As the nucleophilic addition reaction of L_2 with Cys progresses, the supramolecular nature of L_2 changes dramatically, as demonstrated by SEM.

RESULTS AND DISCUSSION

Synthesis of L_1. The simple Diels–Alder adduct L_1 was synthesized in five steps starting from *p*-*tert*-butylphenol as shown in Scheme 1. L_1 and the precursors were well-characterized by ^{1}H and ^{13}C NMR spectroscopy and HRMS (sections SI01–SI05 in the Supporting Information).

Fluorescence Studies of L_1 with AAs and BTs. The reactions of L_1 with amino acids (AAs) and BTs were monitored by fluorescence spectroscopy in acetonitrile by exciting the solutions at 340 nm and measuring the emission intensity. Though the dansyl-conjugated furan precursor P_4 (Scheme 1) is highly emissive, the fluorescence is weakened when the same binds to DMAD covalently to give L_1 as a result of photoinduced electron transfer from the excited state of the fluorophore to the LUMO of the maleate moiety of the Diels–Alder adduct. This is commonly found in the literature in case of maleimide–dye pairs.[11]

When 5 μM solutions of L_1 in acetonitrile were titrated with naturally occurring AAs, no significant changes were observed in the fluorescence intensity except for Cys (Figure 1a and section SI06 in the Supporting Information). In case of Cys, the fluorescence of the dansyl moiety was restored at 520 nm, resulting in high signal-to-noise ratio for the fluorogenic sensing of thiol nucleophiles. Upon addition of 1 equiv of Cys to L_1, i.e., at a 1:1 ratio of Diels–Alder reactive site to nucleophile, the emission band at 520 nm gradually increased as a function of time and finally attained the highest intensity within ~20 min with an overall enhancement of 11 ± 1 fold (Figure 1a,b). A similar result was observed when L_1 was treated with Hcy (Figure 1a,c), and hence L_1 cannot differentiate between Cys and Hcy. In the presence of GSH, no fluorescence enhancement was observed with L_1. The reactions of L_1 with Cys and Hcy were monitored by ^{1}H NMR spectroscopy and ESI MS. Visual color was observed only in the case of Cys among all the naturally occurring AAs under irradiation with UV light (Figure 1a).

^{1}H NMR and ESI MS Studies of L_1 with BTs. In the ^{1}H NMR spectrum of L_1 (Figure 2a), the signal present at 5.7 ppm corresponds to $H_{a'}$ whereas the resonances observed at ~7.2 and 7.35 ppm correspond to the double-bond protons $H_{b'}$ and $H_{c'}$, respectively. The latter are shifted to 6.35 and 6.30 ppm, respectively, upon reaction of L_1 with 1 equiv of Cys, and the peak corresponding to $H_{a'}$ shifts to 5.0 ppm (Figure 2b). The ESI MS spectrum shows a peak at m/z = 785.3 corresponding

dx.doi.org/10.1021/jo5021213 | J. Org. Chem. 2014, 79, 10477–10486

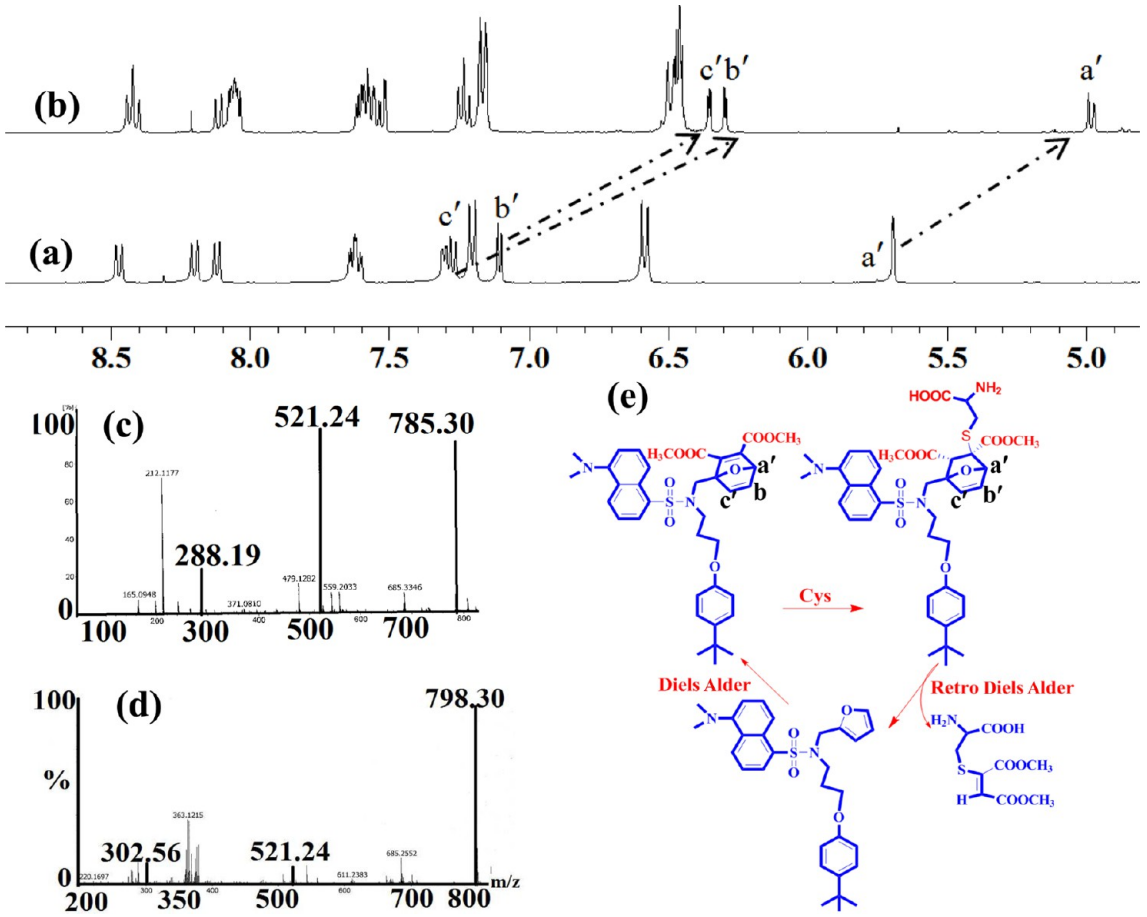

Figure 2. ^{1}H NMR spectra for (a) $\mathbf{L_1}$ and (b) $\mathbf{L_1}$ + 1 equiv of Cys in DMSO-d_6. (c) ESI MS spectra for $\mathbf{L_1}$ + 1 equiv of Cys. (d) ESI MS spectra for $\mathbf{L_1}$ + 1 equiv of Hcy. (e) Proposed reaction scheme for $\mathbf{L_1}$ with Cys.

to the {$\mathbf{L_1}$ + Cys} adduct (Figure 2c). A retro-Diels–Alder product was also observed at m/z = 521.2, and the concomitant byproduct $\mathbf{P_{11}}$ was observed at m/z = 288. Thus, both the NMR and mass spectra support the attack of Cys at the double bond present in the OND moiety in $\mathbf{L_1}$ (Figure 2d). Similar reactivity between $\mathbf{L_1}$ and Hcy was observed, and the corresponding adduct formed was seen from the ESI MS peak at m/z = 798.3 (Figure 2e). The observed similarity in the reactivities of $\mathbf{L_1}$ toward Cys and Hcy demonstrates the nonselectivity of $\mathbf{L_1}$, preventing its use as a probe to differentiate these two BTs. However, the reactivity provided encouragement to go for a modified or derivatized version to achieve better selectivity. As the Diels–Alder adduct present in $\mathbf{L_1}$ reacts with thiols but does not differentiate one from the other, several such units may be grafted onto a calixarene platform to take the advantage of their cumulative effect. Such a design was expected on one hand to increase the sensitivity of the fluorescence because of the simultaneous availability of more such centers on the platform and on the other hand to increase the selectivity as a result of the steric crowding of the arms on the calix[6]arene platform.

Grafting the Diels–Alder Adduct onto a Calix[6]arene Platform To Bring Selectivity toward Thiols. In the present case, three $\mathbf{L_1}$ units were brought together onto a calix[6]arene platform to give the 1,3,5-tris derivative $\mathbf{L_2}$ as an improved receptor molecular system. $\mathbf{L_2}$ was synthesized in six steps as shown in Scheme 2. The intermediates[12] and final product were characterized (sections SI07–SI12 in the Supporting Information).

2D COSY and 2D NOESY Analyses of $\mathbf{P_{10}}$ and $\mathbf{L_2}$. Derivatizations at the 1-, 3-, and 5-positions in $\mathbf{P_{10}}$ and $\mathbf{L_2}$ were studied by 2D COSY and NOESY (Figure 3 and section SI13 in the Supporting Information). In the COSY spectrum of $\mathbf{P_{10}}$, correlations were observed between H_4 and H_3, between H_2 and H_3, and between H_{1eq} and H_{1ax}, as revealed by Figure 3a. On the other hand, upon addition of DMAD to $\mathbf{P_{10}}$, two doublets appeared at 3.97 and 4.49 ppm for the H_5 protons, since the C_1 position becomes chiral in $\mathbf{L_2}$ upon the formation of the Diels–Alder adduct (Figure 3c). The bridging protons in $\mathbf{L_2}$ showed two doublets of doublets. On the basis of the NOESY spectra, the bridge protons H_6 in $\mathbf{L_2}$ are correlated with H_2 and H_1 (Figure 3d), whereas in the case of $\mathbf{P_{10}}$ they are correlated only with H_2 (Figure 3b).

Fluorescence Studies of $\mathbf{L_2}$ with AAs and BTs. The reactions of $\mathbf{L_2}$ (5 μM) with BTs and AAs at various mole ratios were monitored by fluorescence spectroscopy in acetonitrile by exciting the solutions at 340 nm. Upon addition of 3 equiv of Cys to $\mathbf{L_2}$ (i.e., a stoichiometric ratio of reactive sites vs nucleophile), the emission band at 520 nm gradually increased as time progressed, and the highest intensity was attained in 22–24 min with an overall enhancement of 12 ± 1 fold (Figure 4a,b). Similar studies were carried out with 10, 15, and 20 equiv of Cys, and the highest intensity was reached in 6–7 min (Figure 4c–e). In the case of Hcy, no fluorescence enhancement was observed up to 10 equiv. However, at 15 and 20

dx.doi.org/10.1021/jo5021213 | J. Org. Chem. 2014, 79, 10477–10486

Scheme 2[a]

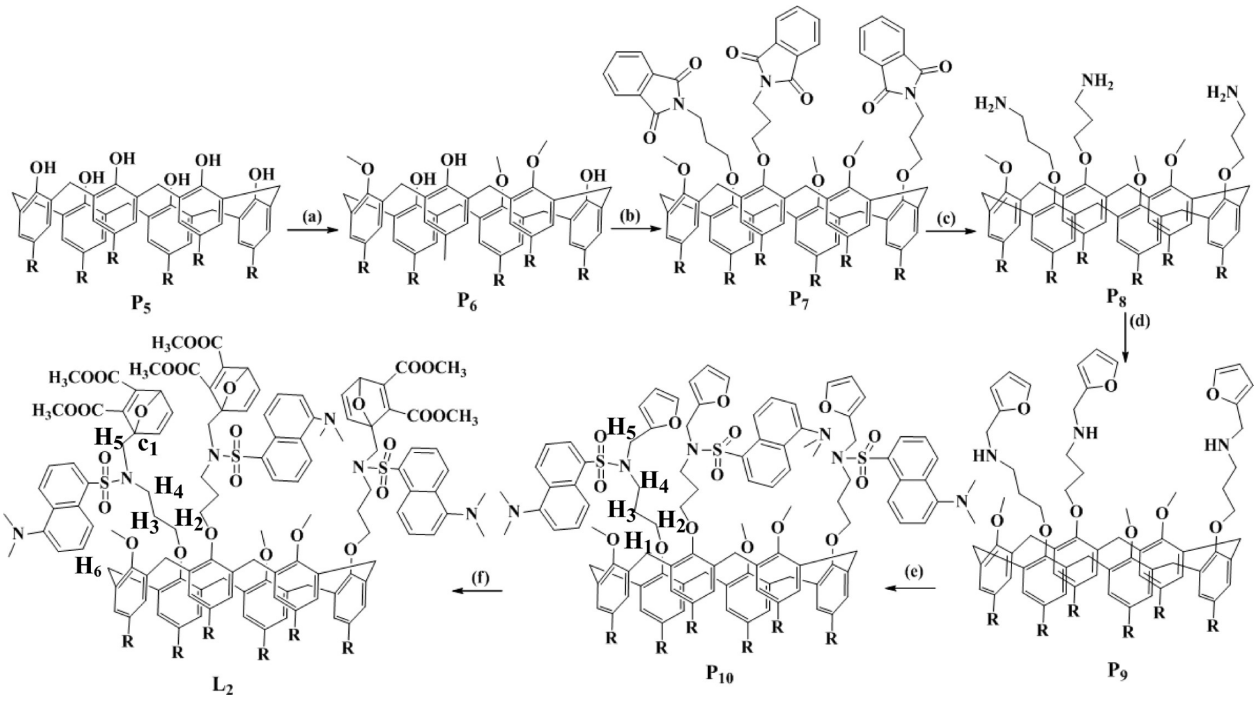

[a]R = *tert*-butyl. Reagents and conditions: (a) CH_3I, K_2CO_3, dry acetone, 70 °C, 5.5 bar, 24 h; (b) 3-bromopropyl phthalimide, Cs_2CO_3, K_2CO_3, CH_3CN, 70 °C, 24 h; (c) NH_2-NH_2, C_2H_5OH, 80 °C, 12 h; (d) furfural, $NaBH_4$, CH_3OH, 24 h, rt; (e) dansyl chloride, Et_3N, from 0 °C to rt, 12 h; (f) DMAD, dry CH_2Cl_2, 55 °C, 24 h.

equiv, the highest intensity was attained in 22−24 min, but it was much lower than that for Cys even at 20 equiv of Hcy, suggesting that all of the centers in $\mathbf{L_2}$ are not reacted with Hcy. This was confirmed when Cys was added 25 min after the addition of Hcy (Figure 4f).

The maximum intensity attained in case of Hcy is one-fourth of that of Cys at 15 equiv and about two-thirds that of Cys at 20 equiv. Though Cys and Hcy differ only by a $-CH_2$ group, their reactivities with $\mathbf{L_2}$ differ, and this is attributable to the steric crowding surrounding the electrophilic center present in $\mathbf{L_2}$. A similar study with GSH did not show any significant fluorescence enhancement even in the presence of 50 equiv with $\mathbf{L_2}$ (section SI14 in the Supporting Information). Thus, the fluorescence enhancements at any given mole ratio are in the order Cys ≫ Hcy ⋙ GSH, suggesting that $\mathbf{L_2}$ is highly selective toward Cys over the other two BTs (Figure 4g,h). A similar study extended to all of the remaining naturally occurring AAs (section SI14 in the Supporting Information) showed no enhancement in the emission intensity of $\mathbf{L_2}$. This was further demonstrated by checking the visual fluorescence color formed in the presence of different AAs, where a distinct color change was found only in the case of the reaction with Cys and not with the other AAs (Figure 4b).

Cys-Induced Supramolecular Features Revealed by SEM. Since the conjugates of calixarenes are known to form supramolecular species and these are sensitive toward binding or reactivity, monitoring of the changes that occur in the supramolecular nature of $\mathbf{L_2}$ in the presence of reactants (viz., Cys) was expected to reveal the progress of the Diels−Alder reaction and also any unusual structures that would form. SEM images were taken in order to observe the morphological changes of the species formed in the reaction mixture consisting of $\mathbf{L_2}$ and Cys at three different mole ratios (Figure 5). $\mathbf{L_2}$ alone showed spherical features with sizes of 80 ± 20 nm, and the morphology differed as the reaction progressed. The reaction mixture containing $\mathbf{L_2}$ and Cys showed species with morphological features consisting of flowerlike, fiberlike, and cabbagelike nanostructures as the mole ratio was changed from 1:1 to 1:3 to 1:5, respectively. The reaction mixture consisting of 1:1 $\mathbf{L_2}$:Cys showed fibrous structures that were further aggregated to form flowerlike ones and spread over 10 to 12 μm.

As the mole ratio was changed from 1:1 to 1:3 by increasing the concentration of Cys, more fibrous structures were seen, and these tended to aggregate to result in flowerlike structures and were also seen as flowers stuck to the branches. From Figure 5k, it was observed that the fibers were transformed into sheetlike structures. When the concentration of Cys was further increased from a mole ratio of 1:3 to 1:5, species resembling the features of cut cabbage were observed, which were surrounded by the sheetlike structures. As the reaction proceeded over a period of time at $\mathbf{L_2}$:Cys = 1:1, the spherical particles that were formed initially aggregated together to transform into fibers and then into sheets (Figure 6). These were further self-assembled to form flowerlike structures over further period of time. Thus, time-dependent aggregational and morphological features were noticed as the reaction between $\mathbf{L_2}$ and Cys progressed, as demonstrated by SEM. In the case of $\mathbf{L_2}$ treated with GSH, no such aggregational features were observed (section SI15 in the Supporting Information), suggesting that GSH does not easily react with $\mathbf{L_2}$. Thus, even the microscopy features are well-suited to differentiate the reactivity of Cys with $\mathbf{L_2}$ from that of GSH.

Cell Imaging and Flow Cytometry Studies of $\mathbf{L_2}$ with Cys. In order to evaluate the sensitivity of $\mathbf{L_2}$ to detect physiologically relevant levels of Cys in living cells, assays were

dx.doi.org/10.1021/jo5021213 | J. Org. Chem. 2014, 79, 10477−10486

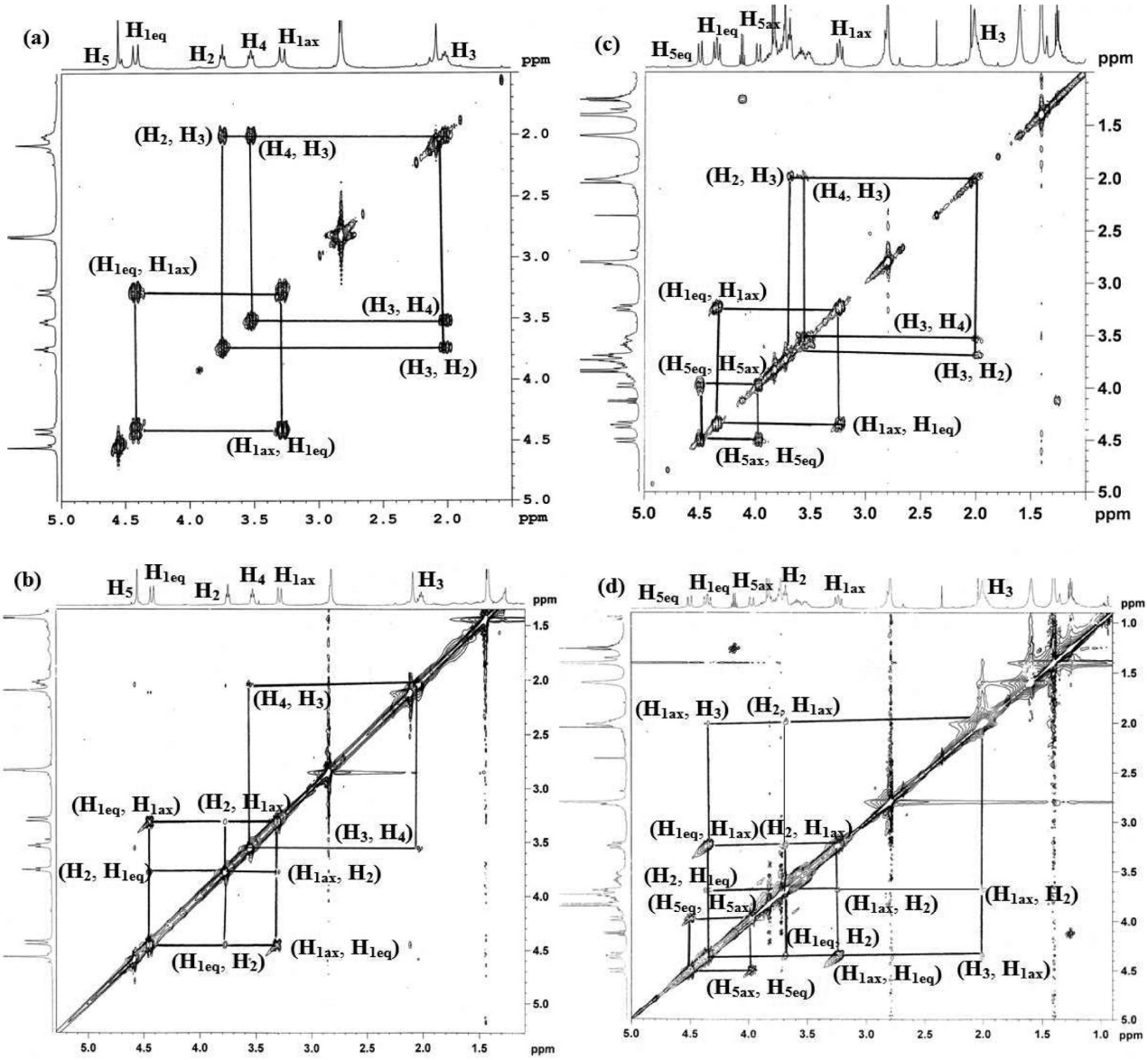

Figure 3. 2D NMR spectra in $CDCl_3$ solvent for (a, b) $\mathbf{P_{10}}$ and (c, d) $\mathbf{L_2}$: (a, c) $^1H-^1H$ COSY; (b, d) $^1H-^1H$ NOESY. Details are given in the Experimental Section.

performed. HeLa cells were incubated with a solution of $\mathbf{L_2}$ (5 μM, 1:99 v/v DMSO/PBS, pH 7.4) for 15 min at 37 °C. The results suggested that $\mathbf{L_2}$ is cell-permeable and reacts with intracellular thiols, resulting in strong fluorescence emission (Figure 7a–c). In order to prove that the probe $\mathbf{L_2}$ is specific to intracellular thiols, *N*-ethylmaleimide (NEM) was used to pretreat the cells to remove the intracellular thiols prior to incubation of the cells with $\mathbf{L_2}$. In this case, no significant intracellular fluorescence was observed (Figure 7d–f), as expected since the pretreatment using NEM resulted in the removal of all of the thiols. Flow cytometry measurements were performed to determine the quenching effect on cells using NEM. A Jurkat E6 cell suspension was treated with 30 μL of 1 M NEM for 45 min in a 5% CO_2 incubator. Then 5 μL of $\mathbf{L_2}$ was added, and the mixture was incubated for 15 min, after which the fluorescence of cells at this stage was compared with that of non-NEM-treated cells. As expected, the cells treated with NEM displayed low fluorescence compared with the untreated ones (Figure 7g). All of these results suggest that $\mathbf{L_2}$ is cell-permeable and shows effective intracellular fluorescence emission upon interaction with thiols inside the cell, which in turn does not show its fluorescence intensity upon pretreatment with NEM.

■ CONCLUSIONS AND CORRELATIONS

A new OND-linked conjugate of calix[6]arene, $\mathbf{L_2}$, has been synthesized and characterized by various spectral techniques. $\mathbf{L_2}$ showed greater sensitivity toward the reaction with Cys compared with Hcy and GSH, and the emission intensities follow the order Cys ≫ Hcy ⋙ GSH. The selectivity mainly comes from the sterically hindered electrophilic center and calix[6]arene platform. This is clearly evident from a comparison of the results for $\mathbf{L_2}$ with those for the reference molecule $\mathbf{L_1}$. $\mathbf{L_2}$ showed selectivity toward the reaction with Cys among the naturally occurring 20 AAs by switch-on green fluorescence (λ_{em} = 520 nm) with an overall enhancement of 12 ± 1 fold. Therefore, $\mathbf{L_2}$ can be used to detect Cys

dx.doi.org/10.1021/jo5021213 | J. Org. Chem. 2014, 79, 10477–10486

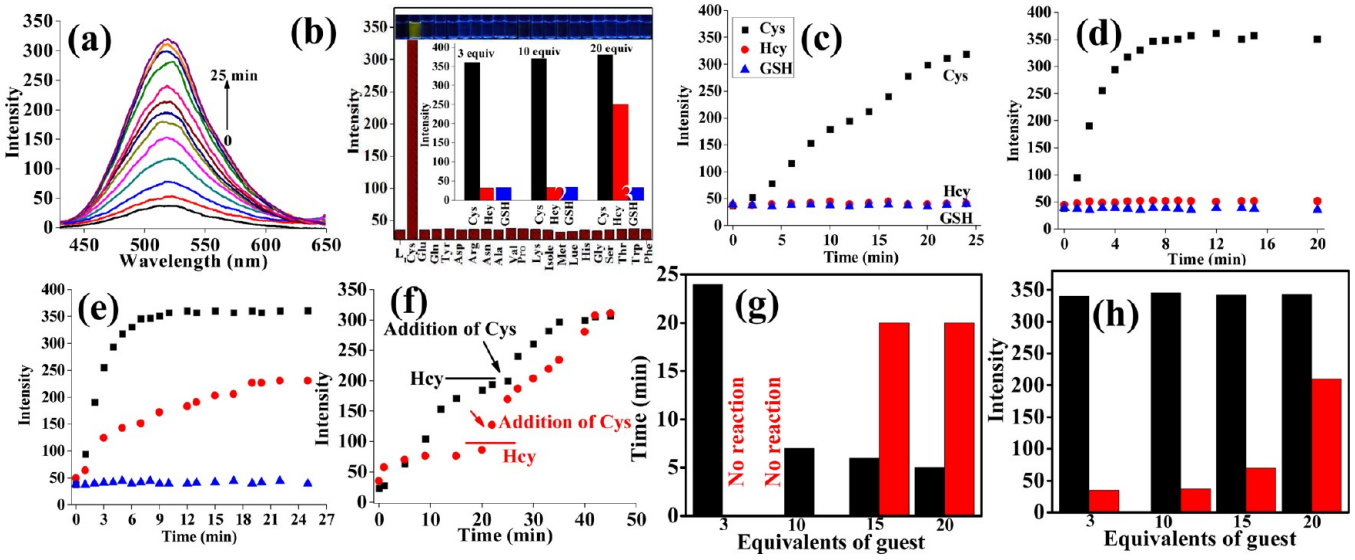

Figure 4. (a) Time-dependent fluorescence spectra for $\mathbf{L_2}$ with 3 equiv of Cys up to 25 min. (b) Histogram showing the fluorescence intensities for various AAs at 1:10 mole ratio after 20 min. Inset (vials): colorimetric titration of $\mathbf{L_2}$ (5 μM) with different AAs (80 μM) in acetonitrile under 365 nm light. Inset (histograms): fluorescence intensities of $\mathbf{L_2}$ in the presence of Cys, Hcy, or GSH at 3, 10, or 20 equiv. (c–e) Plots of fluorescence intensity vs time for titrations of $\mathbf{L_2}$ with Cys, Hcy, or GSH at (c) 3 equiv, (d) 10 equiv, and (e) 20 equiv. (f) Plots of intensity vs time for 15 (red) and 20 equiv (black) of Hcy followed by the addition of 10 equiv of Cys at the 25th minute. (g, h) Histograms showing (g) the time taken to reach the highest intensity and (h) the intensity for Cys (black) and Hcy (red) vs number of equivalents of guest.

stoichiometrically by switch-on fluorescence among the three BTs studied, viz., Cys, Hcy, and GSH.

The reactivity between $\mathbf{L_2}$ with Cys was monitored by SEM, which showed that upon incremental addition of Cys, the spherical particles of $\mathbf{L_2}$ turn to a flowerlike morphology. However, such aggregations were not observed from the reaction of GSH with $\mathbf{L_2}$. Thus, microscopy can differentiate Cys from GSH when $\mathbf{L_2}$ is employed, making it useful in detecting the biothiols. All of these results clearly suggest that there is definite involvement of the calix[6]arene platform and the steric crowding surrounding the electrophilic center. Thus, $\mathbf{L_2}$ can be used for the selective detection of Cys when low concentrations of Hcy are present, and at higher amounts of Hcy, simultaneous detection of Cys and Hcy is possible. Even high concentrations of GSH are not a deterrent for Cys detection as the reaction of the former does not make any contribution to the fluorescence. The practical utility of $\mathbf{L_2}$ was shown by HeLa cells using fluorescence microscopy, which can be used in cellular imaging.

The role of the calix[6]arene platform and the selectivity of $\mathbf{L_2}$ for Cys over Hcy and GSH have been proven by fluorescence studies, while the same studies showed non-selectivity for these thiols by the reference molecule $\mathbf{L_1}$. Even at 10 equiv of biothiol, Hcy and GSH do not contribute to the fluorescence intensity of $\mathbf{L_2}$. However, Cys alone showed high fluorescence intensity with $\mathbf{L_2}$, and this was attained within 6–7 min. Thus, the presence of Hcy and GSH does not hamper the detection of Cys by their reactions with $\mathbf{L_2}$, and hence, $\mathbf{L_2}$ is suitable for use in biological cells. Cys, Hcy, and GSH can also be differentiated by SEM owing to their differential nanostructural features when treated with $\mathbf{L_2}$.

EXPERIMENTAL SECTION

All of the HRMS spectra were measured by the Q-TOF method, and the NMR spectra (including COSY and NOESY) were measured at 500 MHz.

Synthesis and Characterization of $\mathbf{P_1}$. A mixture of *p-tert*-butylphenol (0.50 g, 3.3 mmol), Cs_2CO_3 (2.16 g, 6.6 mmol), and K_2CO_3 (0.92 g, 6.6 mmol) in 40 mL of dry acetonitrile was stirred for 15 min at room temperature, and 3-bromopropylphthalimide (1.43 g, 6.6 mmol) was added. The reaction mixture was heated to 90 °C for 24 h under an atmosphere of N_2. The reaction mixture was brought to room temperature, and the solvent was evaporated to dryness. Water (50 mL) was added to this residue, and the compound was extracted with $CHCl_3$ (3 × 50 mL). The combined organic layers were washed with brine (2 × 50 mL) and dried over Na_2SO_4, and the solvent was removed under reduced pressure. Addition of acetonitrile to this resulted in pure colorless solid product $\mathbf{P_1}$ (0.70 g, 62% yield). Mp 82–86 °C. **^{1}H NMR** ($CDCl_3$, 400 MHz, δ ppm): 1.28 (s, 9H, $-C(CH_3)_3$), 2.17 (quin, 2H, $-CH_2-CH_2-CH_2-$, J = 6.4 Hz), 3.90 (t, 2H, $-NCH_2-$, J = 6.8 Hz), 4.01 (t, 2H, $-OCH_2-$, J = 6.4 Hz), 6.75 (d, 2H, Ar-*H*, J = 8.8 Hz), 7.25 (d, 2H, Ar-*H*, J = 8.8 Hz), 7.71 (dd, 2H, Phth-*H*, J_1 = 3.2 Hz, J_2 = 2.4 Hz), 7.83 (dd, 4H, Phth-*H*, J_1 = 3.2 Hz, J_2 = 2.4 Hz). **^{13}C NMR** ($CDCl_3$, 100 MHz, δ ppm): 28.6 ($-C(CH_3)_3$), 31.7 ($-CH_2-$Phth), 34.2 ($-C(CH_3)_3$), 35.8 ($-CH_2-$N-Phth), 65.8 ($-O-CH_2$), 114.2, 123.4, 126.3, 132.3, 134.1, 143.6, 156.7 (Ar-*C*, Phth-*C*), 168.6 (*C*=O). **HRMS**: calcd for $C_{21}H_{23}NO_3Na$ [M + Na^+] 360.1570, found 360.1569. **FTIR** (KBr, cm^{-1}): 1713 ($\nu_{C=O}$), 2961 (ν_{C-H}).

Synthesis and Characterization of $\mathbf{P_2}$. Hydrazine monohydrate (1.48 mL, 15.00 mmol) was added to a solution of compound $\mathbf{P_1}$ (0.5 g, 1.5 mmol) in ethanol (20 mL). The reaction mixture was refluxed for 12 h and then cooled to room temperature. Water (50 mL) was added, and the resulting precipitate was extracted using $CHCl_3$ (3 × 50 mL). The organic extracts were combined and dried over Na_2SO_4. After filtration, removal of the solvent under reduced pressure afforded pure *p-tert*-butylphenylamine $\mathbf{P_2}$ as a white solid (0.22 g, 71% yield). Mp 65–69 °C. **^{1}H NMR** ($CDCl_3$, 400 MHz, δ ppm): 1.29 (s, 9H, $-C(CH_3)_3$), 1.91 (quin, 2H, $-CH_2-CH_2-CH_2-$, J = 6.0 Hz), 2.90 (t, 2H, $-NCH_2-$, J = 6.8 Hz), 4.03 (t, 2H, $-OCH_2-$, J = 6.0 Hz), 6.84 (d, 2H, Ar-*H*, J = 8.8 Hz), 7.29 (d, 2H, Ar-*H*, J = 8.8 Hz). **^{13}C NMR** ($CDCl_3$, 100 MHz, δ ppm): 31.7 ($-C(CH_3)_3$), 31.3 ($-C(CH_3)_3$), 34.2 ($-CH_2-CH_2-CH_2-$), 39.5 ($-NCH_2-CH_2-CH_2O-$), 65.9 ($-NCH_2-CH_2-CH_2O-$), 114.0, 126.3, 143.4, 156.8 (Ar-*C*). **HRMS**: calcd for $C_{13}H_{22}NO$ [M^+] 208.1696, found 208.1694. **FTIR** (KBr, cm^{-1}): 2962 (ν_{C-H}), 3409 (ν_{NH_2}).

dx.doi.org/10.1021/jo5021213 | J. Org. Chem. 2014, 79, 10477–10486

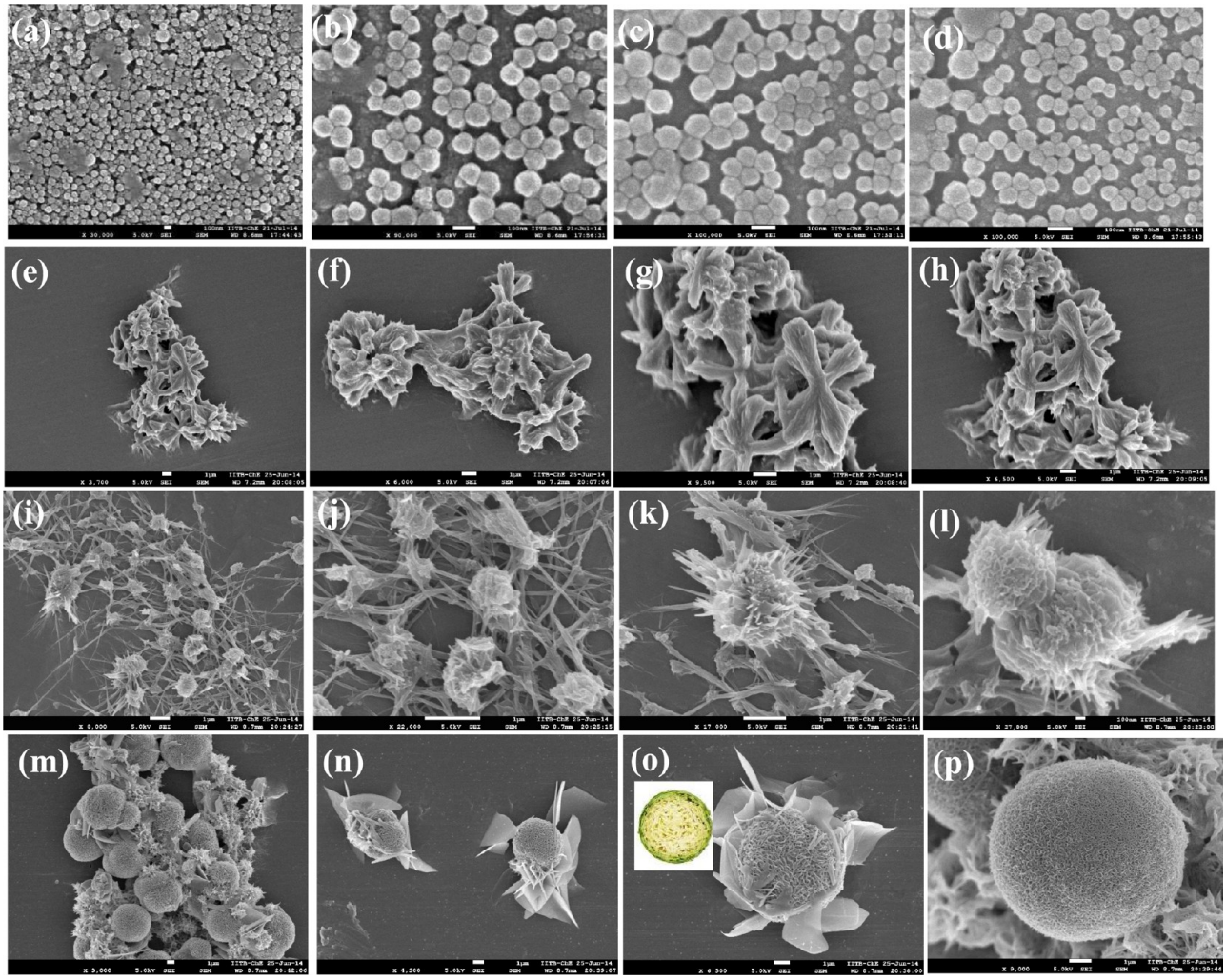

Figure 5. SEM images of (a–d) $\mathbf{L_2}$ and (e–p) $\mathbf{L_2}$ and Cys as a function of $\mathbf{L_2}$:Cys mole ratio: (e–h) $\mathbf{L_2}$:Cys = 1:1; (i–l) $\mathbf{L_2}$:Cys = 1:3; (m–p) $\mathbf{L_2}$:Cys = 1:5.

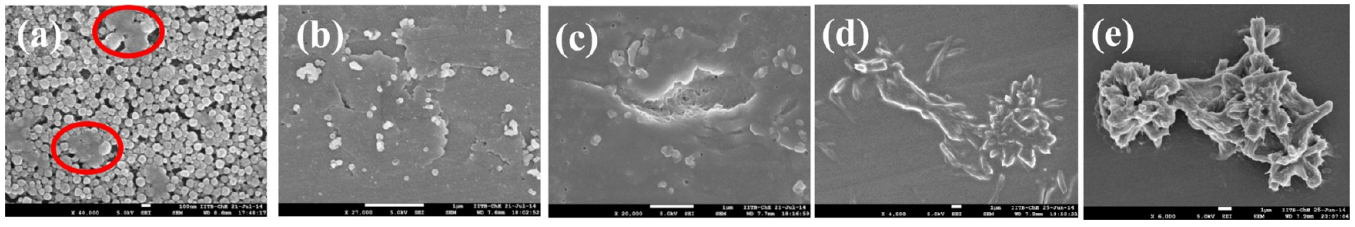

Figure 6. SEM images of (a) $\mathbf{L_2}$ and (b–e) $\mathbf{L_2}$ with 1 equiv of Cys at 10, 20, 30, and 45 min, respectively.

Synthesis and Characterization of $\mathbf{P_3}$. A mixture of $\mathbf{P_2}$ (0.13 g, 0.10 mmol) and furfural (0.06 g, 0.6 mmol) was stirred in 20 mL of dry methanol for 12 h under an atmosphere of N_2. $NaBH_4$ (0.03 g, 6.4 mmol) was added to this reaction mixture, which was then further stirred for 3 h at room temperature and evaporated to dryness. Water (30 mL) was added, and the resulting mixture was extracted with $CHCl_3$ (3 × 25 mL). All of the organic extracts were combined and dried over Na_2SO_4. The organic layers were filtered, and the solvent was evaporated to provide the product, which was used in the next step without further purification. The product was initially liquid but after some time became a viscous semisolid (0.14 g, 98% yield). **^{1}H NMR** ($CDCl_3$, 400 MHz, δ ppm): 1.30 (s, 9H, $-C(CH_3)_3$), 1.96 (quin, 2H, $-CH_2-CH_2-CH_2-$, J = 6.5 Hz), 2.80 (t, 2H, $-NCH_2-$, J = 6.5 Hz), 3.79 (s, 2H, Furan$-CH_2$), 4.01 (t, 2H, $-OCH_2-$, J = 6.0 Hz), 6.17 (d, 1H, Furan-*H*, J = 2.5 Hz), 6.31 (td, 2H, Furan-*H*, J_1 = 15.0 Hz, J_2 = 1.5 Hz), 6.84 (d, 2H, Ar-*H*, J = 9.0 Hz), 7.29 (d, 2H, Ar-*H*, J = 9.0 Hz). **^{13}C NMR** ($CDCl_3$, 125 MHz, δ ppm): 29.7 ($-CH_2-CH_2-CH_2-$), 31.7 ($-C(CH_3)_3$), 34.1 ($-C(CH_3)_3$), 46.3 ($-N-CH_2$), 57.1 (Furan$-CH_2-$), 66.3 ($-O-CH_2$), 107.0, 110.2, 110.4, 114.0, 114.0, 126.3, 141.9, 142.6, 143.3, 143.4, 153.9, 156.7 (Ar-C, Furan-Ar-*C*). **HRMS**: calcd for $C_{18}H_{26}NO_2$ [M^+] 288.1958, found 288.1955. **FTIR** (KBr, cm^{-1}): 1514 ($\nu_{C=C}$), 2962 (ν_{C-H}).

Synthesis and Characterization of $\mathbf{P_4}$. To a stirred solution of $\mathbf{P_3}$ (0.6 g, 2.0 mmol) in CH_2Cl_2 (10 mL) was added triethylamine (0.64 mL, 4.1 mmol) via syringe under N_2. The solution was stirred for 15 min, and 5-dimethylaminonaphthalenesulfonyl chloride (0.67 g, 2.5 mmol) in dry CH_2Cl_2 (5 mL) was added. The resulting solution was stirred for 14 h at room temperature, and the reaction mixture was poured into 1.0 M pH 7.4 phosphate buffer (10 mL). The organic phase was washed with water (2 × 15 mL), dried over Na_2SO_4, and concentrated. The pure product was obtained by column chromatography carried out on silica gel (1:10 EtOAc/hexane) as a yellow-green

dx.doi.org/10.1021/jo5021213 | J. Org. Chem. 2014, 79, 10477–10486

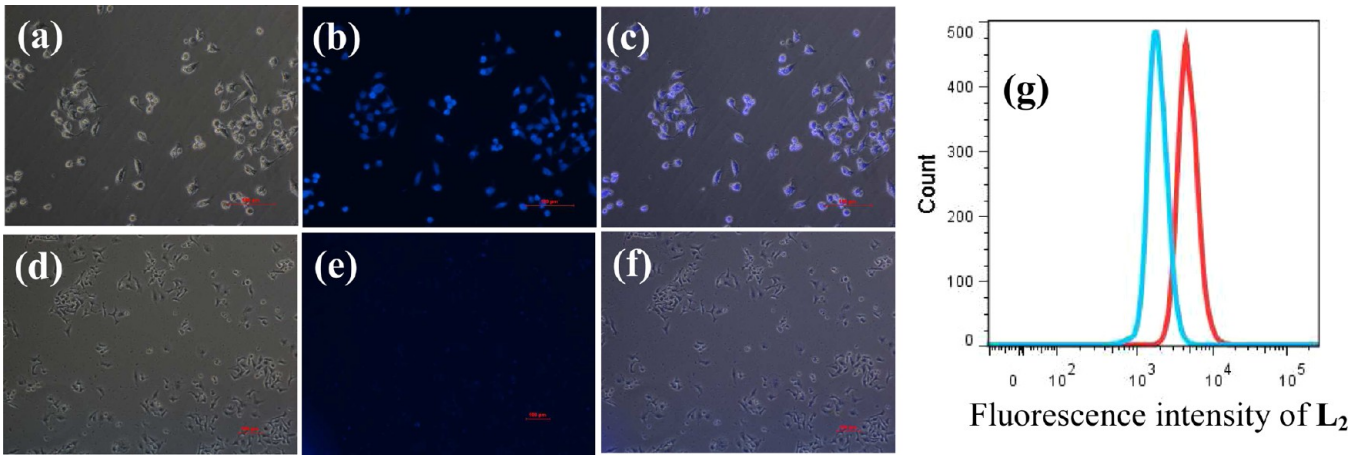

Figure 7. Fluorescence images obtained at 20× magnification from HeLa cells (excitation at λ_{max} = 340−380 nm and emission at λ_{max} = 435−485 nm). (a) Bright-field image of HeLa cells treated with L_2 (5 μL). (b) Fluorescence image of the cells in (a). (c) Merged image of (a) and (b). (d) Bright-field image of HeLa cells treated with 1 M NEM followed by addition of L_2 (5 μL). (e) Fluorescence image of the cells in (d). (f) Merged image of (d) and (e). (g) Flow cytometry graphs for cells treated with NEM followed by addition of L_2 (blue) and cells treated with only L_2 (red).

oil that solidified upon storage (0.75 g, 69% yield). **^{1}H NMR** ($CDCl_3$, 400 MHz, δ ppm): 1.28 (s, 9H, −C(CH_3)$_3$), 1.89 (quin, 2H, −CH_2−CH_2−CH_2−, J = 6.4 Hz), 2.87 (s, 6H, −N(CH_3)$_2$), 3.41 (t, 2H, −NCH_2−, J = 6.8 Hz), 3.67 (t, 2H, −OCH_2−, J = 6.4 Hz), 4.56 (s, 2H, Furan−CH_2−N−), 6.16 (d, 1H, Furan-*H*, J = 3.2 Hz), 6.23 (dd, 1H, Furan-*H*, J_1 = 2.0 Hz, J_2 = 1.2 Hz), 6.58 (d, 2H, Ar-*H*, J = 8.8 Hz), 7.16 (d, 1H, Dansyl-*H*, J = 7.6 Hz), 7.22 (d, 2H, Ar-*H*, J = 8.8 Hz), 7.45 (t, 1H, Dansyl-*H*, J = 7.6 Hz), 7.50 (t, 1H, Dansyl-*H*, J = 7.6 Hz), 8.12 (dd, 1H, Dansyl-*H*, J_1 = 1.2 Hz, J_2 = 7.6 Hz), 8.28 (d, 1H, Dansyl-*H*, J = 8.8 Hz), 8.48 (d, 1H, Dansyl-*H*, J = 8.4 Hz). **^{13}C NMR** ($CDCl_3$, 125 MHz, δ ppm): 27.8 (−CH_2−CH_2−CH_2−), 31.7 (−C(CH_3)$_3$), 34.2 (−C(CH_3)$_3$), 43.2 (−N−CH_2), 44.4 (Furan−CH_2−), 45.5 (−N(CH_3)$_2$), 64.9 (−O−CH_2), 109.9, 110.6, 113.9, 115.2, 119.6, 123.2, 126.2, 128.2, 129.9, 130.1, 130.2, 130.2, 130.6, 134.9, 142.7, 143.4, 149.9, 151.9, 156.5 (Ar-*C*, Dansyl-Ar-*C*, Furan-Ar-*C*). **HRMS**: calcd for $C_{30}H_{36}N_2SO_4Na$ [M + Na^+] 543.2288, found 543.2289. **FTIR** (KBr, cm^{-1}): 1143 ($\nu_{S=O}$), 1324 ($\nu_{S=O}$), 2950 (ν_{C-H}).

Synthesis and Characterization of L_1. A mixture of P_4 (0.30 g, 0.57 mmol) and dimethyl acetylenedicarboxylate (0.16 g, 1.15 mmol) was dissolved in dry CH_2Cl_2 (2 mL). The solvent was removed under a stream of N_2 at 60 °C, and the reaction mixture was heated with stirring at 70−75 °C until the P_4 was consumed as determined by TLC. The reaction mixture was dissolved in a minimal amount of hot toluene, loaded directly onto a prepacked silica gel chromatography column, and eluted with 1:10 hexane/EtOAc to afford a light-yellow solid (0.20 g, 52% yield). Mp 110−114 °C. **^{1}H NMR** ($CDCl_3$, 400 MHz, δ ppm): 1.28 (s, 9H, −C(CH_3)$_3$), 1.89 (quin, 2H, −CH_2−CH_2−CH_2−, J = 1.4 Hz), 2.88 (s, 6H, −N(CH_3)$_2$), 3.48 (quin, 2H, −NCH_2−, J = 1.6 Hz), 3.64 (quin, 2H, −OCH_2−, J = 1.6 Hz), 3.78 (s, 3H, −COOCH_3), 3.84 (s, 3H, −COOCH_3), 3.98 (d, Diels−Alder adduct −CH_{2eq}, J = 12.8 Hz), 4.49 (d, Diels−Alder adduct −CH_{2ax}, J = 12.8 Hz), 5.54 (d, 1H, Furan-*H*, J = 1.2 Hz), 6.59 (d, 2H, Ar-*H*, J = 8.5 Hz), 7.11 (d, 1H, Furan-*H*, J = 1.5 Hz), 7.13 (d, 1H, Furan-*H*, J = 1.2 Hz), 7.17 (d, 1H, Dansyl-*H*, J = 7.0 Hz), 7.21 (d, 2H, Ar-*H*, J = 8.5 Hz), 7.48 (dd, 1H, Dansyl-*H*, J_1 = 0.8 Hz, J_2 = 6.0 Hz), 7.50 (dd, 1H, Dansyl-*H*, J_1 = 0.8 Hz, J_2 = 6.0 Hz), 8.20 (dd, 1H, Dansyl-*H*, J_1 = 1.2 Hz, J_2 = 5.6 Hz), 8.33 (d, 1H, Dansyl-*H*, J = 6.8 Hz), 8.50 (d, 1H, Dansyl-*H*, J = 6.8 Hz). **^{13}C NMR** ($CDCl_3$, 125 MHz, δ ppm): 27.3 (−CH_2−CH_2−CH_2−), 31.7 (−C(CH_3)$_3$), 34.2 (−C(CH_3)$_3$), 45.6 (−N−CH_2), 46.1 (−N(CH_3)$_2$), 52.6 (Furan−CH_2−), 52.8 (COOCH_3), 65.2 (−O−CH_2), 84.0 (Furan-CH), 97.9 (Furan-chiral-*C*), 113.9, 115.3, 119.6, 123.3, 126.2, 128.4, 130.1, 130.2, 130.2, 130.7, 134.7, 143.3, 143.9, 144.6, 152.0, 152.9, 154.1, 156.6 (Ar-*C*, Dansyl-Ar-*C*, Furan-Ar-*C*), 162.9 (−COOCH$_3$), 164.2 (−COOCH$_3$). **HRMS**: calcd for $C_{36}H_{42}N_2SO_8Na$ [M + Na^+] 685.2554, found 685.2550. **FTIR** (KBr, cm^{-1}): 1138 ($\nu_{S=O}$), 1324 ($\nu_{S=O}$), 1715 ($\nu_{C=O}$), 2954 (ν_{C-H}).

Synthesis and Characterization of P_6. To a mixture of *p-tert*-butylcalix[6]arene P_5 (1.0 g, 1 mmol) and K_2CO_3 (0.426 g, 3 mmol) in 70 mL of dry acetone was added methyl iodide (0.27 mL, 4 mmol). The entire reaction was carried out in an autoclave at 70 °C by pressurizing the solution to 5.5 kg/cm^2 for 24 h. At this stage, both the pressure and temperature were brought to normal, and the reaction mixture was filtered off by rejecting the residuals, after which the solvent was evaporated. Finally, the solid residue was dissolved in 100 mL of CH_2Cl_2 and washed with water (2 × 50 mL) and saturated brine. The pure compound was obtained as pure white color flacks (0.42 g, 40% yield) by silica gel column chromatography using 1:24 THF/hexane as the eluent. **^{1}H NMR** ($CDCl_3$, 400 MHz, δ ppm): 1.0 (s, 27H, −C(CH_3)$_3$), 1.2 (s, 27H, −C(CH_3)$_3$), 3.4 (s, 9H, OCH_3), 3.9 (s, 12H, Ar−CH_2−Ar), 6.8 (s, 3H, Ar−O*H*), 6.9 (s, 6H, Ar-*H*), 7.0 (s, 6H, Ar-*H*). **^{13}C NMR** ($CDCl_3$, 100 MHz, δ ppm): 29.6, 29.9, 29.9, 30.5, 31.2, 31.7, 32.1 (−C(CH_3)$_3$), 34.0, 34.2 (−C(CH_3)$_3$), 61.6 (−O−CH_3), 125.8, 125.9, 126.8, 132.6, 142.5, 147.0, 150.0, 152.5 (Ar-*C*). **HRMS**: calcd for $C_{69}H_{90}O_6$ [M + K]$^+$ 1053.6369, found 1053.6359. **FTIR** (KBr, cm^{-1}): 2960 (ν_{C-H}), 3326 (ν_{-OH}).

Synthesis and Characterization of P_7. According to a modified literature procedure, a mixture of 1,3,5-trimethoxycalix[6]arene P_6 (0.50 g, 0.49 mmol), Cs_2CO_3 (0.96 g, 2.90 mmol), and K_2CO_3 (0.41 g, 2.90 mmol) in 50 mL of dry acetonitrile was stirred for 15 min at room temperature, and then 3-bromopropylphthalimide (0.65 g, 2.9 mmol) was added. The resultant mixture was heated to 80−90 °C for 24 h under an atmosphere of N_2. Upon completion of the reaction as determined by TLC, the reaction mixture was brought to room temperature. The solvent was evaporated to dryness, and water (100 mL) was added. The solution was extracted with $CHCl_3$ (3 × 70 mL), and the organic fraction was washed with brine (2 × 50 mL) and dried over Na_2SO_4. The solvent was removed under reduced pressure, and finally acetonitrile was added to obtain pure colorless solid product P_7 (0.65 g, 84% yield). **^{1}H NMR** ($CDCl_3$, 400 MHz, δ ppm): 0.75 (s, 27H, −C(CH_3)$_3$), 1.38 (s, 27H, −C(CH_3)$_3$), 2.08 (s, 9H, OCH_3), 2.30 (quin, 6H, J = 6.8 Hz), 3.38 (d, 6H, Ar−CH_{2eq}−Ar, J = 15.20 Hz), 3.99 (quin, 12H, −OCH_2 + −NCH_2, J = 7.2 Hz), 4.53 (d, 6H, Ar−CH_{2ax}−Ar, J = 15.8 Hz), 6.59 (s, 6H, Ar-*H*), 7.24 (s, 6H, Ar-*H*), 7.71 (dd, 4H, Phth-*H*, J_1 = 3.04 Hz, J_2 = 2.4 Hz), 7.86 (dd, 4H, Phth-*H*, J_1 = 3.00 Hz, J_2 = 2.4 Hz). **^{13}C NMR** ($CDCl_3$, 100 MHz, δ ppm): 29.7, 29.8 (Ar−CH_2−Ar), 31.2, 31.3, 31.7 (−C(CH_3)$_3$), 31.8 (−CH_2−Phth), 34.0, 34.3 (−C(CH_3)$_3$), 35.9 (−CH_2−N-Phth), 60.2 (−O−CH_3), 70.9 (−O−CH_2), 123.4, 123.5, 123.3, 128.1, 132.3, 133.1, 133.7, 134.0, 145.7, 151.9, 154.6 (Ar-*C*), 168.49 (C═O). **HRMS**: calcd for $C_{102}H_{117}N_3O_{12}K$ [M + K]$^+$ 1615.8308, found 1615.8322. **FTIR** (KBr, cm^{-1}): 1245 ($\nu_{C=O\ imide}$), 1714 ($\nu_{C=O\ imide}$), 2961 (ν_{C-H}).

Synthesis and Characterization of P_8. Hydrazine monohydrate (1.0 mL, 190.00 mmol) was added to a solution of compound P_7 (0.3

dx.doi.org/10.1021/jo5021213 | J. Org. Chem. 2014, 79, 10477−10486

g, 0.19 mmol) in ethanol (20 mL). The reaction mixture was refluxed for 12 h and then cooled to room temperature. Water (50 mL) was added, and the resulting precipitate was extracted with $CHCl_3$ (3 × 50 mL). The organic phase was washed with water (3 × 50 mL) and dried with Na_2SO_4. After filtration, evaporation of the solvent under reduced pressure afforded pure calix[6]tris(amine) as a brownish-white solid (0.17 g, 75% yield). **^{1}H NMR** ($CDCl_3$, 400 MHz, δ ppm): 0.87 (s, 27H, $-C(CH_3)_3$), 1.33 (s, 27H, $-C(CH_3)_3$), 1.92 (t, 6H, $-CH_2-CH_2-CH_2-$, J = 6 Hz), 2.37 (s, 9H, OCH_3), 2.95 (t, 6H, $-NCH_2-$, J = 6 Hz), 3.8–4.2 (br, 12H, $-CH_{2eq}$ + $-CH_{2ax}$), 3.88 (t, 6H, $-O-CH_2$, J = 6 Hz), 6.73 (s, 6H, Ar-*H*), 7.22 (s, 6H, Ar-*H*). **^{13}C NMR** ($CDCl_3$, 100 MHz, δ ppm): 30.0, (Ar$-CH_2-$Ar), 31.3, 31.7 ($-C(CH_3)_3$), 33.9 ($-CH_2-$Phth), 34.1, 34.3 ($-C(CH_3)_3$), 39.6 ($-CH_2-$N-Phth), 60.3 ($-O-CH_3$), 71.1 ($-O-CH_2$), 124.4, 127.4, 133.2, 133.6, 145.8, 145.9, 152.1, 154.2 (Ar-*C*). **HRMS**: calcd for $C_{78}H_{112}N_3O_6$ $[M + H]^+$ 1186.8546, found 1186.8506. **FTIR** (KBr, cm^{-1}): 1481 (ν_{CH_2}), 1588 ($\nu_{N-H\ ben}$), 2961 (ν_{C-H}), 3374 (ν_{N-H}).

Synthesis and Characterization of P_9. A mixture of calix[6]-tris(amine) P_8 (0.13 g, 0.10 mmol) and furfural (0.06 g, 0.6 mmol) was added to 20 mL of dry CH_3OH. The reaction mixture was allowed to stir for 12 h, and then $NaBH_4$ (0.03 g, 6.4 mmol) was added. The mixture was allowed to stir for another 3 h. Upon completion of the reaction (as checked by TLC), the organic layer was evaporated to dryness. Water (30 mL) was added, and the resulting mixture was extracted with $CHCl_3$ (3 × 25 mL). The organic layer was dried over Na_2SO_4, filtered, and evaporated to get the product as a brown semipaste material (0.13 g, 86% yield), which was used in the next step without further purification. **^{1}H NMR** ($CDCl_3$, 400 MHz, δ ppm): 0.77 (s, 27H, $-C(CH_3)_3$), 1.39 (s, 27H, $-C(CH_3)_3$), 2.06 (quin, 6H, $-CH_2-CH_2-CH_2-$, J = 6.4 Hz), 2.16 (s, 9H, $-OCH_3$), 2.94 (t, 6H, $-NCH_2-$, J = 6.8 Hz), 3.39 (d, 6H, Ar$-CH_{2eq}-$Ar, J = 15.20 Hz), 3.81 (s, 6H, Furan$-CH_2-$N$-$), 3.98 (t, 6H, $-OCH_2-$, J = 6.0 Hz), 4.55 (d, 6H, Ar$-CH_{2eq}-$Ar, J = 15.20 Hz), 6.17 (d, 3H, Furan-*H*, J = 3.1 Hz), 6.28 (dd, 3H, Furan-*H*, J_1 = 1.2 Hz, J_2 = 1.2 Hz), 6.63 (s, 6H, Ar-*H*), 7.27 (s, 6H, Ar-*H*), 7.32 (d, 3H, Furan-*H*, J = 1.6 Hz). **^{13}C NMR** ($CDCl_3$, 100 MHz, δ ppm): 29.8, (Ar$-CH_2-$Ar), 30.9, 31.3, 31.8 ($-C(CH_3)_3$), 31.8 ($-CH_2-CH_2-$), 34.1, 34.4 ($-C(CH_3)_3$), 46.5, 46.8 ($-CH_2-$Furan), 60.2 ($-O-CH_3$), 71.3 ($-O-CH_2$), 107.0, 110.2, 123.6, 128.1, 133.3, 133.8, 141.9, 145.7, 145.9, 151.9, 154.1, 154.6 (Ar-*C*, Furan-Ar-*C*). **HRMS**: calcd for $C_{93}H_{124}N_3O_9$ $[M + H]^+$ 1426.9332, found 1426.9371. **FTIR** (KBr, cm^{-1}): 1485 (ν_{CH_2}),1645 ($\nu_{-N-H\ ben}$), 2961 (ν_{C-H}), 3364 (ν_{N-H}).

Synthesis and Characterization of P_{10}. To a stirred solution of P_9 (0.9 g, 0.6 mmol) in CH_2Cl_2 (10 mL) was added triethylamine (0.62 mL, 2.2 mmol) via syringe under N_2. The solution was stirred for 15 min, and then 5-dimethylaminonaphthalenesulfonyl chloride (0.6 g, 2.2 mmol) in dry CH_2Cl_2 (5 mL) was added. The resulting solution was stirred for 24 h at room temperature, and the reaction mixture was poured into 1.0 M pH 7.4 phosphate buffer (20 mL). The organic phase was washed with water (2 × 15 mL), dried over Na_2SO_4, and concentrated. The pure product was obtained as a yellow-green oil that solidified upon storage (0.95 g, 70% yield) after column chromatography carried out with silica gel (0–25% EtOAc/hexanes). **^{1}H NMR** ($CDCl_3$, 500 MHz, δ ppm): 0.76 (s, 27H, $-C(CH_3)_3$), 1.41 (s, 27H, $-C(CH_3)_3$), 2.01 (quin, 6H, $-CH_2-CH_2-CH_2-$, J = 7 Hz), 2.08 (s, 9H, OCH_3), 2.85 (s, 18H, $-N(CH_3)_2$), 3.27 (d, 6H, Ar$-CH_{2eq}-$Ar, J = 15.0 Hz), 3.52 (t, 6H, $-NCH_2-$, J = 7.0 Hz), 3.74 (t, 6H, $-OCH_2-$, J = 6.5 Hz), 4.41 (d, 6H, Ar$-CH_{2eq}-$Ar, J = 15.0 Hz), 4.55 (s, 6H, Fur$-CH_2-$N$-$), 6.15 (d, 3H, Furan-*H*, J = 3.5 Hz), 6.17 (dd, 3H, Furan-*H*, J_1 = 2.5 Hz, J_2 = 2.5 Hz), 6.58 (s, 6H, Ar-*H*), 7.11 (d, 3H, Dansyl-*H*, J = 7.5 Hz), 7.21 (m, 3H, Furan-*H*, J = 1.0 Hz), 7.26 (s, 6H, Ar-*H*), 7.44 (t, 3H, Dansyl-*H*, J = 8.0 Hz), 7.48 (t, 3H, Dansyl-*H*, J = 8.0 Hz), 8.12 (d, 3H, Dansyl-*H*, J = 7.5 Hz), 8.30 (d, 3H, Dansyl-*H*, J = 8.5 Hz), 8.48 (d, 3H, Dansyl-*H*, J = 8 Hz). **^{13}C NMR** ($CDCl_3$, 125 MHz, δ ppm): 28.9 ($-CH_2-CH_2-CH_2-$), 29.7, 29.8 (Ar$-CH_2-$Ar), 29.8, 31.2, 31.3 ($-C(CH_3)_3$), 31.7, 31.8, 34.0, 34.4 ($-C(CH_3)_3$), 45.0 ($-N-CH_2$), 45.5 ($-N(CH_3)_2$), 60.1 ($O-CH_3$), 70.6 ($-O-CH_2$), 109.9, 110.7, 115.2, 119.6, 123.5, 128.1, 128.2, 129.7, 130.1, 130.2, 130.4, 133.5, 135.1, 142.8, 145.7, 145.9, 151.9, 151.8, 154.5 (Ar-*C*, Dansyl-Ar-*C*, Furan-Ar-*C*). **HRMS**: calcd for $C_{129}H_{157}N_6O_{15}S_3$ $[M + H]^+$ 2127.0903, found 2126.0864. **FTIR** (KBr, cm^{-1}): 1144 ($\nu_{SO_2\ symm}$), 1362 ($\nu_{SO_2\ asymm}$), 2961 (ν_{C-H}).

Synthesis and Characterization of L_2. A mixture of P_{10} (0.24 g, 0.11 mmol) and dimethyl acetylenedicarboxylate (0.2 g, 1.4 mmol) was dissolved in dry CH_2Cl_2 (2 mL). The solvent was removed under a stream of nitrogen at 60 °C, and the reaction mixture was heated with stirring at 70–75 °C until the P_{10} was consumed, as determined by TLC. The reaction mixture was dissolved in a minimal amount of hot toluene, loaded directly onto a prepacked silica gel chromatography column, and eluted with 1:4 hexane/EtOAc to afford the product as a light-yellow solid (0.16 g, 57% yield). Mp 125–127 °C. **^{1}H NMR** ($CDCl_3$, 400 MHz, δ ppm): 0.74 (s, 27H, $-C(CH_3)_3$), 1.40 (s, 27H, $-C(CH_3)_3$), 2.00 (br, 15H, $-OCH_3$, $-CH_2-CH_2-CH_2-$), 2.79 (s, 18H, $-N(CH_3)_2$), 3.23 (dd, 6H, Ar$-CH_{2eq}-$Ar, J_1 = 4.8 Hz, J_2 = 8 Hz), 3.53 (m, 6H, $-NCH_2-$), 3.70 (t, 6H, $-OCH_2-$, J = 4 Hz), 3.72 (s, 9H, $-OCH_3$), 3.82 (s, 9H, $-OCH_3$), 3.97 (d, 3H, Diels–Alder adduct $-CH_{2eq}$, J = 16 Hz), 4.34 (dd, 6H, Ar$-CH_{2eq}-$Ar, J_1 = 4.8 Hz, J_2 = 8 Hz), 4.49 (d, 3H, Diels–Alder adduct $-CH_{2ax}$, J = 16 Hz), 4.41 (d, 6H, Ar$-CH_{2eq}-$Ar, J = 15.0 Hz), 5.56 (s, 3H, Furan-*H*), 6.54 (s, 6H, Ar-*H*), 7.07 (s, 6H, Ar-*H*), 7.23 (br, 6H, Furan-*H*), 7.49 (dt, 6H, Dansyl-*H*, J_1 = 24 Hz, J_2 = 16 Hz), 8.20 (d, 3H, Dansyl-*H*, J = 8.0 Hz), 8.34 (d, 3H, Dansyl-*H*, J = 8.0 Hz), 8.47 (d, 3H, Dansyl-*H*, J = 8 Hz). **^{13}C NMR** ($CDCl_3$, 100 MHz, δ ppm): 28.6 ($-CH_2-CH_2-CH_2-$), 29.9 (Ar$-CH_2-$Ar), 31.3, 31.8 ($-C(CH_3)_3$), 34.0, 34.4 ($-C(CH_3)_3$), 45.5 ($-N-CH_2$), 45.9, 46.5 ($-N(CH_3)_2$), 52.4, 52.7 ($-COOCH_3$), 60.1 ($O-CH_3$), 70.9 ($-O-CH_2$), 84.1 (Furan$-CH$), 97.9 (Adduct Chiral *C*), 115.3, 119.6, 123.4, 128.1, 128.4, 130.0, 130.2, 130.7, 133.2, 133.6, 134.9, 143.9, 144.7, 145.6, 145.8, 151.9, 153.0, 154.0, 154.6 (Ar-*C*, Dansyl-Ar-*C*, Furan-Ar-*C*), 162.9, 164.2 ($-COOCH_3$). **HRMS**: calcd for $C_{147}H_{174}N_6O_{27}S_3K$ $[M + K]^+$ 2590.1221, found 2590.1267. **FTIR** (KBr, cm^{-1}): 1138 ($\nu_{SO_2\ symm}$), 1376 ($\nu_{SO_2\ asymm}$), 2968 (ν_{C-H}).

Fluorescence Titration Details. Bulk solutions of L_1 and L_2 were prepared in DMSO, and the amino acids were dissolved initially in the minimum amount of water and then diluted with acetonitrile. The concentration of the bulk solution of L_1 or L_2 and amino acid or Hcy was maintained at 6×10^{-4} M throughout the titration. In the case of GSH, the bulk solution was prepared at a concentration of 6×10^{-3} M, and from this stock solution different mole ratios were added to L_1 or L_2. The fluorescence titrations were carried out by exciting the solution of L_1 or L_2 at 340 nm in a 1 cm quartz cell, maintaining the final $[L_1]$ or $[L_2]$ at 5 μM in a total volume of 3 mL by dilution with acetonitrile.

SEM Sample Preparation. The SEM samples of L_2 and L_2 + Cys were prepared from a solution of L_2 in DMSO at a concentration of 6×10^{-4} M. Cys was initially dissolved in the minimum amount of water, and then the volume was made up with acetonitrile to the desired concentration. The stock solutions of these were sonicated for 10 min. After that the reaction mixture was allowed to stand for around 40 min to facilitate complete reaction, and then a 20 μL aliquot was taken from this stock solution to spread over a piece of aluminum foil using a drop-casting method. The samples were then dried under the IR lamp for 15 min and analyzed.

Cell Culture Studies. HeLa cells and Jurkat E6-1 cells were obtained from the cell repository of the National Center for Cell Sciences (NCCS), India. HeLa cells were grown in DMEM containing 10% FBS. The medium was also supplemented with 1 mM L-glutamine. The cells were seeded in six-well plates and used for the experiments after attaining 70% confluency. Similarly, Jurkat cells were grown in RPMI 1640 medium supplemented with FBS and L-glutamine. Cells were cultured in T25 flasks containing 10 mL of medium. Cells were seeded at 5×10^5 cells/mL in the T flasks. These cultures were kept in a CO_2 incubator maintained at 37 °C and 5% CO_2 under humid conditions.

Fluorescence Microscopy. After reaching 70% confluency, HeLa cells were washed twice with PBS buffer containing 1 mM Ca^{2+} and 1 mM Mg^{2+}, and 1 mL of the same solution was added to the wells. The L_2 stock solution was prepared in DMSO with a concentration of 6×10^{-4} M. L_2 was added into wells to a final concentration of 5 μM.

dx.doi.org/10.1021/jo5021213 | J. Org. Chem. 2014, 79, 10477–10486

Similarly, a positive control was prepared by adding NEM at a final concentration of 1 mM and kept in the CO_2 incubator for 30 min. To the positive control (cells + NEM) well was added 5 μM $\mathbf{L_2}$, and the solution was again kept in the incubator for 15 min. After completion of the incubation period, cells were washed twice with PBS buffer and both florescence and phase-contrast images were captured with a microscope using a 20× objective. To capture fluorescence images, the compound was excited with UV light (340−380 nm) and the signal was captured in the blue range (435−485 nm).

Flow Cytometry. Actively growing Jurkat cells were taken and washed twice with PBS to remove the medium. The cells were washed and resuspended in PBS buffer, maintaining a cell density of 1×10^6 cells/mL. To one tube was added $\mathbf{L_2}$, and the mixture was incubated for 30 min in the CO_2 incubator. To another tube was added NEM, and the mixture was incubated for 30 min; then $\mathbf{L_2}$ was added, and the sample was incubated for 15 min and analyzed. The samples were excited with a UV laser (354 nm), and the signal was captured using a 525/50 nm bandpass filter. Ten thousand events were recorded during the analysis to get statistically significant data.

■ ASSOCIATED CONTENT

Ⓢ Supporting Information

^{1}H and ^{13}C NMR and mass spectral data for $\mathbf{P_1}$, $\mathbf{P_2}$, $\mathbf{P_3}$, $\mathbf{P_4}$, $\mathbf{P_6}$, $\mathbf{P_7}$, $\mathbf{P_8}$, $\mathbf{P_9}$, $\mathbf{P_{10}}$, $\mathbf{L_1}$, and $\mathbf{L_2}$; fluorescence spectra of all AAs with $\mathbf{L_1}$ and $\mathbf{L_2}$; and SEM data for $\mathbf{L_2}$. This material is available free of charge via the Internet at http://pubs.acs.org.

■ AUTHOR INFORMATION

Corresponding Author

*Phone: 91 22 2576 7162. Fax: 91 22 2572 3480. E-mail: cprao@iitb.ac.in.

Notes

The authors declare no competing financial interest.

■ ACKNOWLEDGMENTS

C.P.R. acknowledges the financial support from DST, CSIR, and DAE-BRNS. V.V.S.M. acknowledges CSIR for a fellowship. D.S.Y. acknowledges UGC for her fellowship. We acknowledge SAIF for SEM.

■ DEDICATION

Dedicated to Professor C.N.R. Rao, F.R.S. on the occasion of his 80th birthday.

■ REFERENCES

(1) (a) Wood, Z. A.; Schroder, E.; Harris, R.; Poole, L. B. *Trends Biochem. Sci.* **2003**, *28*, 32. (b) Schulz, J. B.; Lindenau, J.; Seyfried, J.; Dichgans, J. *Eur. J. Biochem.* **2000**, *267*, 4904. (c) Brandes, N.; Schmitt, S.; Jakob, U. *Antioxid. Redox Signaling* **2009**, *11*, 997.

(2) Wang, X. F.; Cynader, M. S. *J. Neurosci.* **2001**, *21*, 3322.

(3) (a) Shahrokhian, S. *Anal. Chem.* **2001**, *73*, 5972. (b) Refsum, H.; Smith, A. D.; Ueland, P. M.; Nexo, E.; Clarke, R.; McPartlin, J.; Johnston, C.; Engbaek, F.; Schneede, J.; McPartlin, C.; Scott, J. M. *Clin. Chem.* **2004**, *50*, 3. (c) Refsum, H.; Ueland, P. M.; Nygård, O.; Vollset, S. E. *Annu. Rev. Med.* **1998**, *49*, 31.

(4) Townsend, T.; Solo-Gabriele, H.; Tolaymat, T.; Stook, K.; Hosein, N. *Soil Sediment Contam.* **2003**, *12*, 779.

(5) (a) Guy, J.; Caron, K.; Dufresne, S.; Michnick, S. W.; Skene, W. G.; Keillor, J. W. *J. Am. Chem. Soc.* **2007**, *129*, 11969. (b) Matsumoto, T.; Urano, Y.; Shoda, T.; Kojima, H.; Nagano, T. *Org. Lett.* **2007**, *9*, 3375.

(6) (a) Wang, W.; Escobedo, J. O.; Lawrence, C. M.; Strongin, R. M. *J. Am. Chem. Soc.* **2004**, *126*, 3400. (b) Lee, M. H.; Yang, Z.; Lim, C. W.; Lee, Y. H.; Dongbang, S.; Kang, C.; Kim, J. S. *Chem. Rev.* **2013**, *113*, 5071. (c) Das, P.; Mandal, A. K.; Chandar, N. B.; Baidya, M.; Harshad, B.; Ganguly, B. B.; Ghosh, S. K.; Das, A. *Chem.—Eur. J.* **2012**, *18*, 15382. (d) Yang, Y.-K.; Shim, S.; Tae, J. *Chem. Commun.* **2010**, *46*, 7766. (e) Xu, H.; Wang, Y.; Huang, X.; Li, Y.; Zhang, H.; Zhong, X. *Analyst* **2012**, *137*, 924. (f) Maeda, H.; Matsuno, H.; Ushida, M.; Katayama, K.; Saeki, K.; Itoh, N. *Angew. Chem., Int. Ed.* **2005**, *44*, 2922. (g) Bouffard, J.; Kim, Y.; Swager, T. M.; Weissleder, R.; Hilderbrand, S. A. *Org. Lett.* **2008**, *10*, 37. (h) Shao, J.; Sun, H.; Guo, H.; Ji, S.; Zhao, J.; Wu, W.; Yuan, X.; Zhang, C.; James, T. D. *Chem. Sci.* **2012**, *3*, 1049. (i) Maity, D.; Govindaraju, T. *Org. Biomol. Chem.* **2013**, *11*, 2098. (j) Tang, B.; Xing, Y.; Li, P.; Zhang, N.; Yu, F.; Yang, G. *J. Am. Chem. Soc.* **2007**, *129*, 11666. (k) Moragues, M. E.; Martínez-Máñez, R.; Sancenón, F. *Chem. Soc. Rev.* **2011**, *40*, 2593. (l) Kand, D.; Kalle, A. M.; Talukdar, P. *Org. Biomol. Chem.* **2013**, *11*, 1691. (m) Huo, F. J.; Sun, Y. Q.; Su, J.; Yang, Y. T.; Yin, C. X.; Chao, J. B. *Org. Lett.* **2010**, *12*, 4756. (n) Chen, X.; Zhou, Y.; Peng, X.; Yoon, J. *Chem. Soc. Rev.* **2010**, *39*, 2120. (o) Jung, H. S.; Chen, X.; Kim, J. S.; Yoon, J. *Chem. Soc. Rev.* **2013**, *42*, 6019. (p) Chen, H.; Zhao, Q.; Wu, Y.; Li, F.; Yang, H.; Yi, T.; Huang, C. *Inorg. Chem.* **2007**, *46*, 11075. (q) Li, H.; Fan, J.; Wang, J.; Tian, M.; Du, J.; Sun, S.; Sun, P.; Peng, X. *Chem. Commun.* **2009**, 5904. (r) Niu, L.-Y.; Guan, Y.-S.; Chen, Y.-Z.; Wu, L.-Z.; Tung, C.-H.; Yang, Q.-Z. *J. Am. Chem. Soc.* **2012**, *134*, 18928. (s) Peng, R.; Lin, L.; Wu, X.; Liu, X.; Feng, X. *J. Org. Chem.* **2013**, *78*, 11602.

(7) Benesch, R. E.; Benesch, R. *J. Am. Chem. Soc.* **1955**, *77*, 5877.

(8) (a) Jiang, X.-D.; Zhang, J.; Shao, X.; Zhao, W. *Org. Biomol. Chem.* **2012**, *10*, 1966. (b) Shibata, A.; Uzawa, T.; Nakashima, Y.; Ito, M.; Nakano, Y.; Shuto, S.; Ito, Y.; Abe, H. *J. Am. Chem. Soc.* **2013**, *135*, 14172.

(9) (a) Liu, J.; Sun, Y.-Q.; Huo, Y.; Zhang, H.; Wang, L.; Zhang, P.; Song, D.; Shi, Y.; Guo, W. *J. Am. Chem. Soc.* **2014**, *136*, 574. (b) Yang, X.-F.; Huang, Q.; Zhong, Y.; Li, Z.; Li, H.; Lowry, M.; Escobedo, J. O.; Strongin, R. M. *Chem. Sci.* **2014**, *5*, 2177. (c) Hong, V.; Kislukhin, A. A.; Finn, M. G. *J. Am. Chem. Soc.* **2009**, *131*, 9986. (d) Gac, S. L.; Zeng, X.; Reinaud, O.; Jabin, I. *J. Org. Chem.* **2005**, *70*, 120.

(10) (a) Hwang, C.; Sinskey, A. J.; Lodish, H. F. *Science* **1992**, *257*, 1496. (b) Chung, T. K.; Funk, M. A.; Baker, D. H. *J. Nutr.* **1990**, *120*, 158. (c) Park, S.; Imlay, J. A. *J. Bacteriol.* **2003**, *185*, 1942.

(11) Girouard, S.; Houle, M. H.; Grandbois, A.; Keillor, J. W.; Michnick, S. W. *J. Am. Chem. Soc.* **2005**, *127*, 559.

(12) (a) Gutsche, C. D.; Dhawan, B.; No, K. H.; Muthukrishnana, R. *J. Am. Chem. Soc.* **1981**, *103*, 3782. (b) Janseen, R. G.; Verboon, W.; Reinhoudt, D. N.; Casnati, A.; Feriks, M.; Pochini, A.; Ugozzoli, F.; Ungaro, R.; Nieto, P. M.; Carramolino, M.; Cuevas, F.; Prados, P.; de Mendoza, J. *Synthesis* **1993**, 380. (c) Gac, S. L.; Zeng, X.; Reinaud, O.; Jabin, I. *J. Org. Chem.* **2005**, *70*, 1204. (d) Mummidivarapu, V. V. S.; Nehra, A.; Hinge, V. K.; Rao, C. P. *Org. Lett.* **2012**, *14*, 2968.